

## Identification of Internal Defects in Forged Shafts by Measurement of Residual Stresses Using X-Ray Method

Kamil Anasiewicz<sup>1</sup>, Jerzy Józwik (0000-0002-8845-0764)<sup>1</sup>, Michał Lelęć (0000-0002-6398-4014)<sup>1</sup>, Paweł Pieśko<sup>1</sup>, Stanisław Legutko (0000-0001-8973-5035)<sup>2</sup>, Janusz Tomczak (0000-0003-3781-1432)<sup>3</sup>, Zbigniew Pater (0000-0001-5504-157X)<sup>3</sup>, Tomasz Bulzak (0000-0002-0525-8321)<sup>3</sup>

<sup>1</sup>Department in Production Engineering, Faculty of Mechanical Engineering, Lublin University of Technology,

<sup>2</sup>Institute of Mechanical Technology, Faculty of Mechanical Engineering, Poznań University of Technology, 20-618 Lublin, Poland

<sup>3</sup>Department of Metal Forming, Faculty of Mechanical Engineering, Lublin University of Technology, 20-618 Lublin, Poland

The present paper discusses important aspects of residual stress measurements in forged shafts with defects using the X-ray method. A random population of shafts was selected for the study, for which, depending on the type of rolling process, turning was performed, measuring stress changes after successive machining passes. In the forged shafts studied, the existence and location of internal defects were identified using computed tomography. The impact of internal defects on the stress distribution on the surface of the machined workpiece was observed. It was observed that the use of the X-ray method to measure residual stresses makes it possible to determine the state of stresses and their distribution, which is crucial for the safety and durability of shaft-type parts, and allows the impact of a defect on the distribution of residual stresses to be identified. On the basis of the results obtained, it was observed that there is a correlation between the occurrence of internal defects in forged shafts and the distribution of residual stresses in characteristic sections along the length of the shaft after machining

**Keywords:** Residual stresses, Forged shafts, Material defects, X-ray method, Cross hatch rolling

### 1 Introduction

One of the causes of the resulting dimensional and shape inaccuracies in machining processes is the state of stress in the part after the manufacturing process and in the absence of external forces. These stresses are referred to in the literature as intrinsic or residual stresses. The modern automotive, engineering and aerospace industries require high precision and reliability of structural components, which implies the necessity of accurate residual stress measurements and precise dimensional and shape evaluation of fabricated components. The dimensional and shape accuracy of fabricated components is closely related to the residual stresses that arise both during the technological process of manufacturing both semi-finished components and the cutting process itself [1, 2]. Technically, all machining processes for manufacturing machine parts lead to residual stresses, and the quality of the machining of precision parts itself is crucial to the performance and fatigue life of the part. In the machining process, deformation caused by residual stress is almost inevitable, if only because of the poor stiffness of the parts and structures. Moreover, residual stresses arise due to uneven plastic deformation in the surface layers during the application of forces in the machining process, caused by local heating of the surface

layer, as well as by phase transformations of the surface, resulting in the formation of numerous structures with different specific volumes [3, 4]. It has been found that residual stresses will further reduce dimensional stability, fatigue strength, creep life and corrosion resistance [5]. On the other hand, residual stresses in semi-finished products originate from various metallurgical and processing processes, e.g. forming, during which various structural defects, e.g. collapses, can be generated that are difficult to detect [6]. Thus, it is crucial to monitor and control these stresses and potential structural defects at all stages of production [7]. Figure 1 presents a scheme of machining error formation in relation to residual stresses.

Appropriate residual stress analysis techniques can be used to identify and assess the stress state and internal defects of the material. Moreover, the correct choice of machining parameters, such as speed, feed rate, depth of cut and the use of appropriate tools and cooling technology, has a significant impact on minimising the development of additional stresses in the workpiece material. During the machining process, tool pressure is applied to the workpiece in the contact zone of the tool, which generates compressive and shear stresses. Surface stresses can also lead to the formation of micro-cracks in the material. A correct machining process should introduce compressive stresses

into the material surface. This is confirmed by the studies of, for example, Fayçal Younes El-Hassar [8] and Young K. [9]. In contrast, tensile stresses in the surface of the workpiece material can be the result of local areas of plastic alteration resulting from improperly selected cutting parameters, tool geometry or a lack of rigidity in the workpieces [10]. Advanced measurement methods are crucial to identify and analyse defects, thereby increasing the safety and durability of

components. Cross hatch forging is one of the advanced plastic material forming technologies widely used in the production of shafts and other axisymmetric components. While the process allows for the efficient and cost-effective production of components with complex shapes, it is also a source of potential internal defects that can affect the mechanical properties and durability of the part.

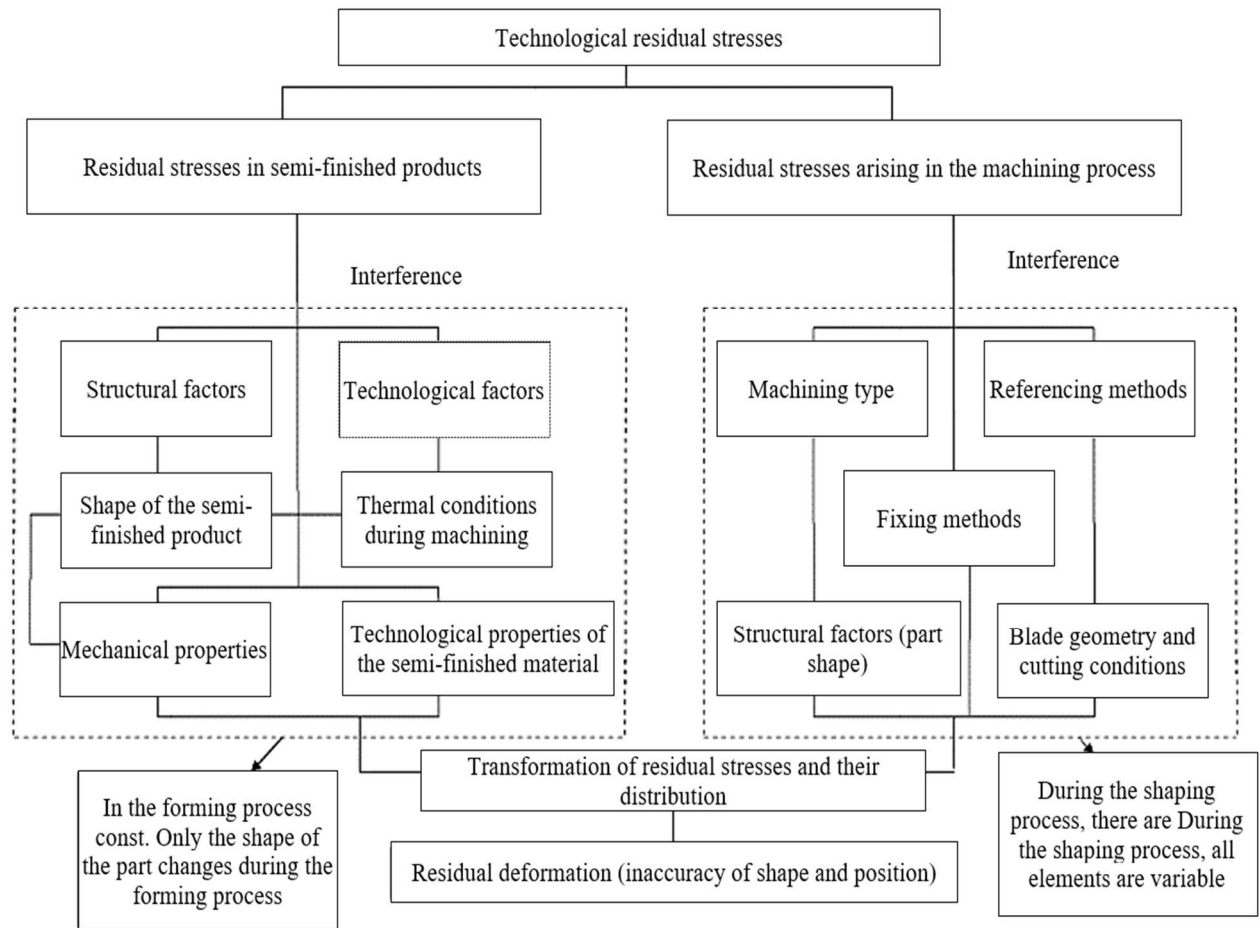


**Fig. 1** Scheme of machining error formation in relation to residual stresses

One of the main problems associated with transverse-symmetric forging is internal defects such as cracks, inclusions, porosity and material inconsistencies [11]. As Zienkiewicz and Bathe [12] observed, during forging, the material is subjected to high plastic deformation, which can lead to microscopic and macroscopic internal discontinuities, especially in areas of stress concentration. These defects are difficult to detect by standard quality control processes, posing the risk of their transformation into major defects during the service life of the product.

Another factor causing the formation of internal defects is the microstructure of the material and its homogenisation. In literature studies, it has been observed that during the cross hatch forging process, inhomogeneities in the microstructure of the material

can lead to local differences in plasticity, which in turn favours the formation of defects such as phase segregation, martensite or trans-crystalline cracks [13]. A study by Wilkha et al. [14] showed that controlling the transverse forging process parameters, such as temperature, strain rate and pressure, is crucial to minimise the risk of internal defects.

Techniques for detecting and assessing internal defects in forged shafts, such as the X-ray method, are essential to ensure the quality and reliability of structural components. Modern methods of examining the internal structure, such as computed tomography or X-ray diffraction, enable accurate mapping of the stress distribution and identification of internal defects at an early stage of production [15, 16].

The measurement of residual stresses is an important part of assessing the strength and durability of structural materials. As observed by Smith [17] and Fitzpatrick and Lodini [18], the X-ray and neutron diffraction methods can be used to precisely determine the stress state, which is essential for assessing the potential failure hazards of materials. Withers [19] emphasises the role of residual stresses in degradation mechanisms, pointing to the need for their accurate analysis in the design and operation processes of structural components. The use of the X-ray method in the analysis of intrinsic stresses makes it possible to accurately determine the distribution of stresses in metallic components, which is crucial for assessing their strength. In the literature, studies by Nowak et al. [20] indicate the high effectiveness of this technique in diagnosing structural defects in forged shafts, highlighting its ability to detect even small defects. Similarly, Kowalski et al. [21] described the use of radiography in stress analysis, pointing out its importance in the context of the durability and reliability of machine components [22]. Industrial metrology plays a key role in quality assurance in manufacturing processes. De Chiffre and colleagues [23] examined the industrial applications of computed tomography, highlighting its importance in the analysis of the internal structure of materials. Phillips and Estler [24] discussed metrology systems used in manufacturing, highlighting their key role in ensuring dimensional and quality compliance.

In summary, the use of the X-ray method and quality control of components contributes to improving the safety and durability of manufactured products. This article aims to present the benefits of integrating X-ray technology methods into the quality analysis of forged shafts [25, 26].

In the research carried out, the focus was on the analysis of residual stresses in forged shafts that contained defects of various types, such as cracks and micro-cracks, internal cavities, dimensional inconsistencies, and shape inconsistencies [27, 28]. Using the X-

ray method, residual stresses were measured after successive turning stages – phases – to investigate the influence of internal defects on the distribution of residual stresses [29].

## 2 Materials and Methods

Within the framework of the conducted research, attention was devoted to the analysis of methods for measuring stresses in the surface layer of the examined component – the forged shaft. The identification and strongly correlated stress-strain relationship in this area is crucial to ensuring the long-term strength and safety of materials in various engineering applications. Figure 2 presents the test object with its geometric parameters constituted in successive machining passes. The forged shaft was made from 42CrMo4 alloy steel. Table 1 shows the chemical composition of the material and Table 2 shows its basic physical properties.

**Tab. 1** Chemical composition of 42CrMo4 alloy steel

Element symbol and content in %	
C	0.418%
Mn	0.770%
Si	0.210%
P	0.010%
S	0.011%
Cr	1.070%
Mo	0.220%

**Tab. 2** Physical properties of 42CrMo4 alloy steel

Property	Value
Density	7.830 g/cm <sup>3</sup>
Young's modulus E	205–209 GPa
Yield strength Re	650–750 MPa
Tensile strength Rm	1050–1180 MPa
Extension A	12–20%

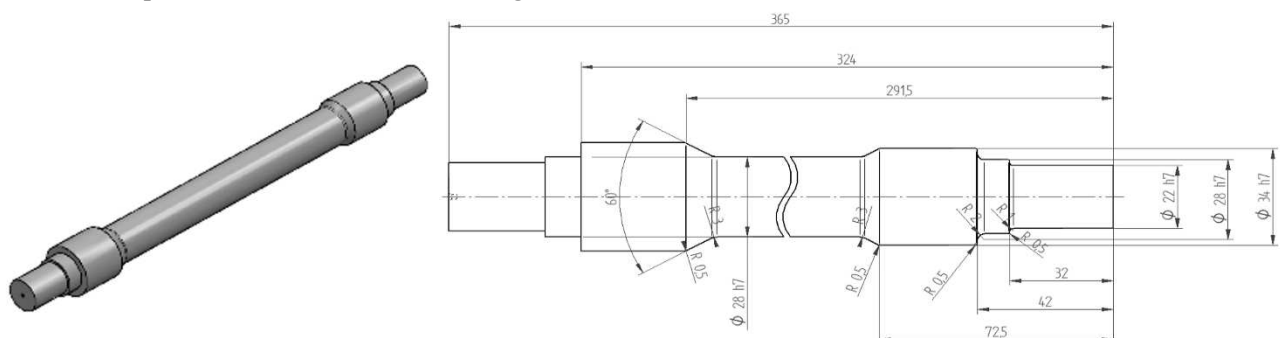


**Fig. 2** Test object: geometric dimensions of the test shaft and 3D geometric model

A Theta-Theta EDGE mobile diffractometer was used to carry out the measurements. Its technical specifications allow precise measurements of residual stresses and analysis of the residual austenite content

of the materials tested. The technical specification of the Theta-Theta EDGE diffractometer is shown below, in Table 3.

**Tab. 3** Technical specifications of the Theta-Theta EDGE diffractometer

Parameter	Specification
Model	EDGE
Goniometer	Angle range: from $-45^{\circ}$ to $+45^{\circ}$ 2-theta angle: from $45^{\circ}$ to $170^{\circ}$
Detector	DECTRIS Mythen Multi Strip Detector
Generator	standard: Cr anode (option: Cu, Mo, W) maximum power: 4W
Collimator	$\varnothing$ 0.5   1   2 mm (standard)
Dimensions and weight of the head	480x330x450 mm; 8.5 kg

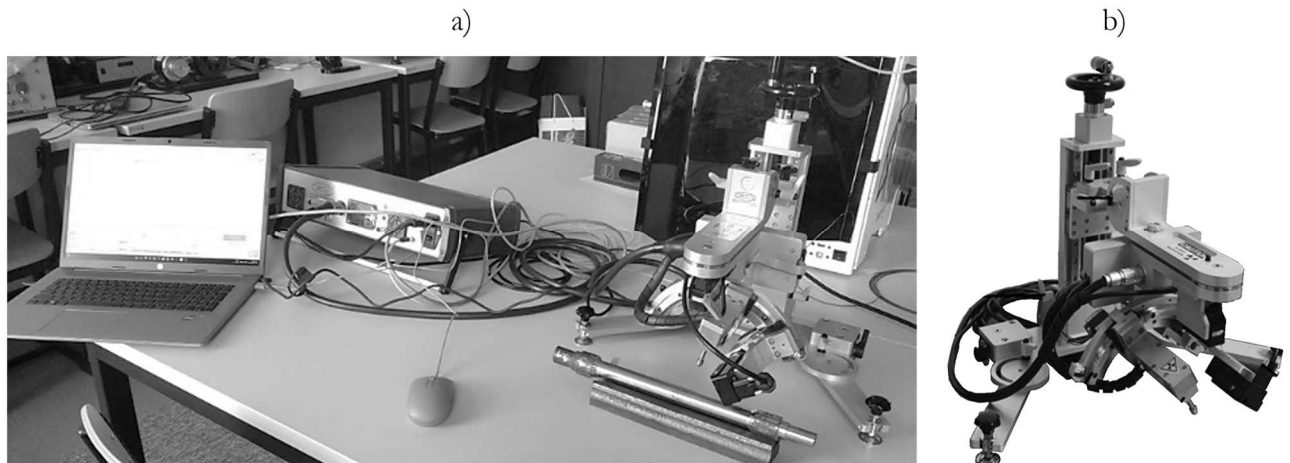
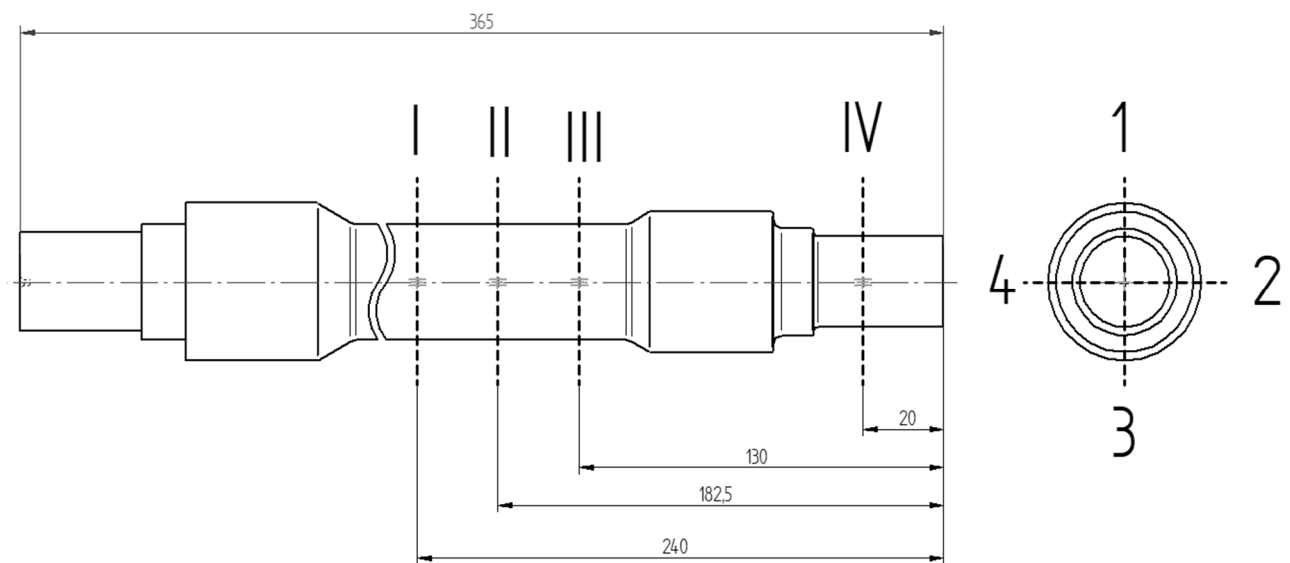
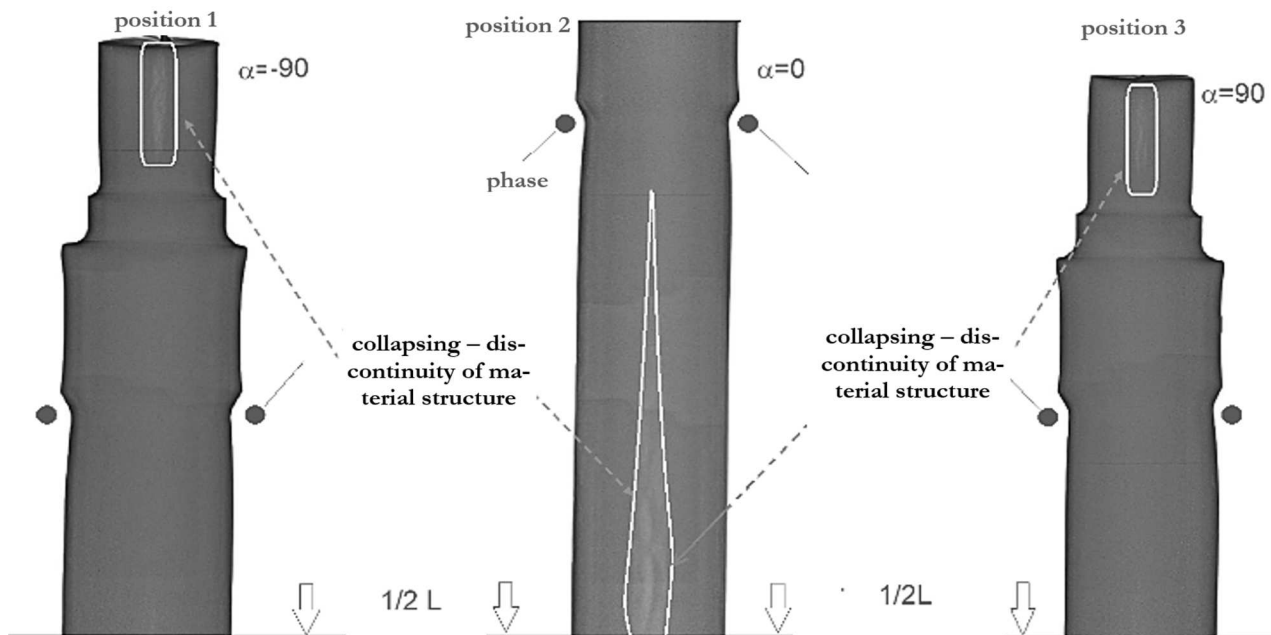
**Fig. 3** Portable Theta-Theta EDGE diffractometer, Manufacturer: GNR, (a) photo of the workstation, (b) photo of the X-ray analyser

Figure 3a shows a view of the workstation and Figure 3b shows a view of the X-ray analyser.

As part of the detailed analysis of the stress state on the surface of the shaft under study, a fixed arrangement of measurement points was adopted, which resulted in a reproducible and precise examination of the stresses in each relevant part of the shaft. This approach involved segmenting the shaft surface into four main cross-sections, designated I, II, III and

IV. This segmentation allows accurate analysis and identification of the homogeneity of the stress in different areas of the shaft, which is crucial for understanding its behaviour under load. For each of the marked sections (I–IV), measurements were taken at four key points, defined on the frontal view of the shaft. These points were numbered 1 to 4, giving a total of 16 measurement points across the shaft.

**Fig. 4** Distribution of measurement points on the shaft



**Fig. 5** Identification of these discontinuity defects in the structure of rolled shafts and their location using computed tomography

The shafts selected for testing have internal defects in the form of cavities – structural internal discontinuities that are not visible from the outside. These defects and their locations were identified using computed tomography (Figure 5).

The research carried out was intended to determine the effect of these structural discontinuities on the mechanical properties of the shafts, and to assess whether or not such internal defects in the shaft can be inferred from the analysis of residual stresses on the surface of pre-machined forged shafts. To assess this, it was decided to perform the shaft turning process in two phases. The process was carried out using constant cutting parameters for each successive layer of material. The turning parameters were as follows: machining speed ( $v_c$ ) was 80 m/min, the depth of cut (ap) was 1 mm, and the feed rate (fn) was 0.12 mm/rot. in the roughing pass and 0.5 mm in the finishing pass with the same feed rate. The cutting insert had a corner radius of 0.4 mm. Shaft clamping on the lathe was carried out by chucking in a three-jaw chuck and supporting with a swivel shank for high lathe machining rigidity. In each phase, successive layers of material as defined above were removed. The study took into account that the turning process introduces stresses into the surface of the workpiece material, but their value is constant for all machined passes and shafts. It was assumed that the differences in residual stress values in the shafts under consideration are the result of internal structural defects present in the shafts.

After the completion of each phase, stress distribution tests were carried out on the newly formed surface using the X-ray diffractometer characterised above.

### 3 Results and Discussion

Figure 6 shows the dependence of the interplanar distance ( $d$  spacings) in crystalline materials as a function of  $\sin(\Psi)^2$ , where:  $\Psi$  – denotes the angle between the normal to the crystallographic plane and the direction of the X-ray beam (in an X-ray diffraction study). The argument axis of the function (X axis) of the graph is represented by  $\sin(\Psi)^2$ . The ordinate axis shows the interplanar spacing ( $d$  spacings) expressed in Angstroms (Å). This distance corresponds to the distance between adjacent crystalline planes in the material and is a key parameter in the identification and characterisation of the material phase and in stress measurements.

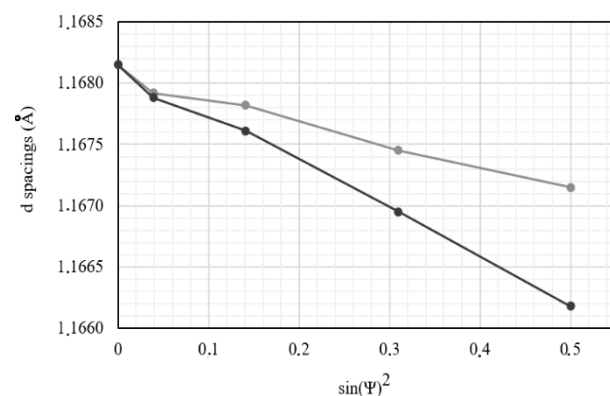


**Fig. 6** The graph shows the relationship between 'd spacings' and  $\sin(\Psi)^2$

In the graph (Fig. 6.), it can be observed that the points line up in a straight line, suggesting a linear relationship between  $d$  and  $\sin(\Psi)^2$  typical of X-ray

diffraction used to measure residual stresses. The inclination of this line reflects the stresses in the material: for alpha-iron, the interplanar spacing on the graph decreases as the angle of incidence of the beam increases, indicating the presence of compressive stresses. These stresses are greater the greater the inclination of the curve. From the graph presented, it can be read that as the angle between the normal to the crystallographic plane and the direction of the X-ray beam  $\sin(\Psi)^2$  increases, the value of the interplanar spacing decreases, which is consistent with the presence of internal stresses in the material under study. In this way, it is possible to assess not only the presence but also the values of stresses in the material, which is important for understanding its mechanical properties.

Figure 7 shows the dependence of the diffraction angle  $2\theta$  ( $2\theta$  being the angle at which X-rays were detected after diffraction) on the angle between the normal to the crystallographic plane and the direction of the X-ray beam ( $\Psi$ ) in an X-ray diffraction study. The shape of the parabola in the graph indicates that the stresses in the material vary as a function of the angle  $\Psi$ . The minimum value of angle  $2\theta$  usually corresponds to a stress-free state. Stress analysis by X-ray diffraction (XRD) is based on the fact that internal stresses in the material affect the interplanar distances in the crystal lattice, which affects the diffraction angle  $2\theta$ .

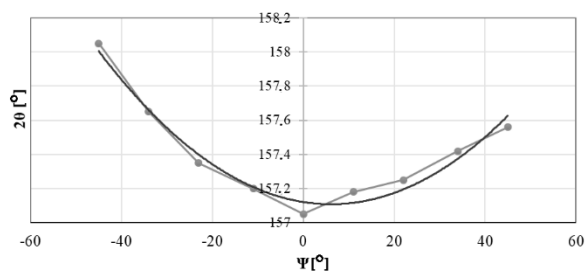


**Fig. 7** Dependence of diffraction angle  $2\theta$  on angle  $\Psi$  of X-ray diffraction

These changes in the interplanar spacing cause shifts in the diffraction angles, which are measurable and can be used to calculate stresses. At zero stresses, the graph would form a horizontal line. The parabolic shape of the graph indicates the presence of stresses, where the bottom of the parabola indicates the value of angle  $2\theta$  for the unstressed state of the material. In contrast, the shape of the parabola allows the value of residual stress to be calculated – deviations from this minimum value indicate the presence of stress. The ‘u’ shape of the parabola indicates the presence of compressive stresses. From this graph, a quantitative analysis of the stresses in the sample can be made by calculating how the diffraction angle  $2\theta$  changes for different crystal orientations ( $\Psi$  values). Using the small-

est squares method, the parabola equation can be fitted to the data points, and the parameters of this fit can be used to calculate the residual stresses in the test material. Figures 8 to 11 show the dependence of the residual stress values that were obtained in the different rolling phases of shafts 1 to 4.

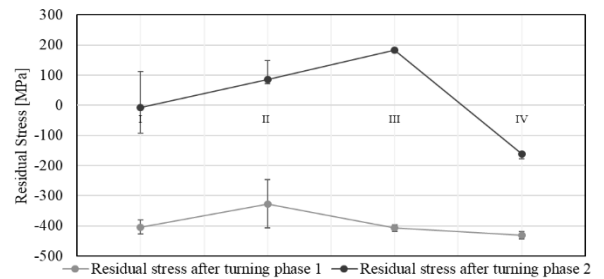


**Fig. 8** Dependence of mean residual stresses for shaft 1 as a function of individual cross-sections I, II, III, IV

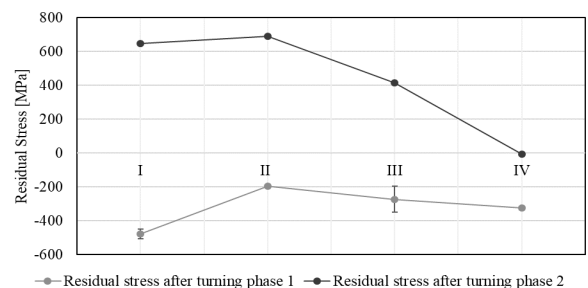


**Fig. 9** Dependence of mean residual stresses for shaft 2 as a function of individual cross-sections I, II, III, IV

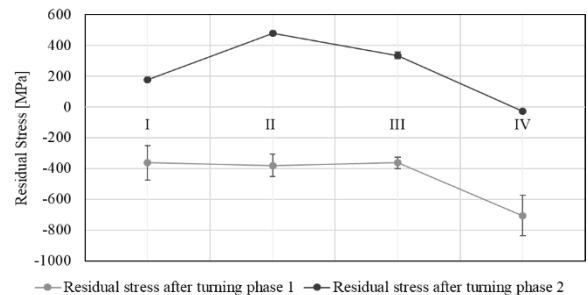


**Fig. 10** Dependence of mean residual stresses for shaft 3 as a function of individual cross-sections I, II, III, IV

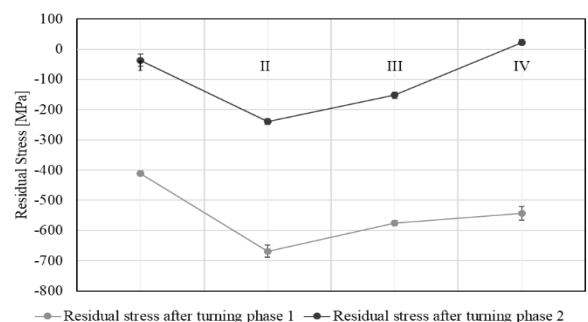


**Fig. 11** Dependence of mean residual stresses for shaft 4 as a function of individual cross-sections I, II, III, IV

The number of turning passes is crucial for the final residual stresses in the material. In cross-sections I, II, and III, the second pass, in shafts with internal

defects, introduces positive tensile stresses, while there are still compressive stresses in cross-section IV, albeit of lower intensity.

**Tab. 4** Summary of average residual stresses in the second section (II) of the shafts marked 'Shaft 1 – Shaft 4'

Shaft number	Stress [MPa]			
	Phase 1	S	Phase 2	S
Shaft 1	-404	26.50	-6.5	100.13
Shaft 2	-379.5	129.59	478.25	123.62
Shaft 3	-195.75	33.52	689	8.26
Shaft 4	-668.75	7.80	-238.75	217.68
S – Standard deviation [MPa]				

**Tab. 5** Comparison of residual stresses in phase 1–2 in sections I–IV in shafts 1–4

Stress [MPa]		
Shaft 1	Phase 1	Phase 2
I	-404.00	6.50
II	-326.50	85.50
III	-407.25	182.75
IV	-430.75	-162.00
Shaft 2	Phase 1	Phase 2
I	-363.00	178.00
II	-379.50	478.25
III	-363.00	335.75
IV	-705.75	-27.25
Shaft 3	Phase 1	Phase 2
I	-478.50	648.25
II	-195.75	689.00
III	-273.25	415.50
IV	-325.75	6.75
Shaft 4	Phase 1	Phase 2
I	-410.75	-36.50
II	-668.75	238.75
III	-575.50	-152.30
IV	-543.25	23.00

Based on the analysis of residual stresses shown in Table 5, for the four forged shafts, three of which have internal defects (Shaft 1, Shaft 2, Shaft 3) and one of which is free of defects (Shaft 4), the following conclusions can be drawn regarding the distribution of compressive and tensile stresses and their influence on the assessment of the presence of internal defects. Compressive (negative) stresses in forged shafts can be beneficial as they help to prevent the initiation of surface cracks. These are usually the result of machining, such as cutting, which introduces surface compression. Tensile (positive) stresses can indicate a potential risk of crack and defect formation, especially when they are unevenly distributed in the material. They may be the result of shaft relaxation and exposure of internal stresses as a result of machining.

The following analysis discusses the average values of shaft stresses for the four cross-sections considered. In shaft 1 in the machining phase 1, the residual

stresses are mostly compressive in all cross-sections, e.g. -404.0 MPa in cross-section I and -430.8 MPa in cross-section IV. In section II, the stresses are lower equal approx. -326.5 MPa, which may suggest the influence of internal defects that reduce the effective stresses in the more deformable parts of the shaft. The change in stresses in machining phase 2, section II from compressive to tensile equal approx. 85.5 MPa after further machining may indicate deformations related to internal defects that are released after material removal. The increase in compressive stress in section IV equal approx. -162.0 MPa suggests that this section, being closest to the support point, tends to accumulate compressive stresses.

In shaft 2, the average compressive stresses in machining phase 1 are dominant in all cross-sections, e.g. -379.5 MPa in cross-section II and -705.8 MPa in cross-section IV. The large standard deviations, especially in cross-section II equal approx. 129.59 MPa,

indicate stress instability, which is characteristic of shafts with internal defects. In machining phase 2, a significant increase in tensile stress is observed in cross-section II equal approx. 478.3 MPa, which can be related to the influence of internal defects on stress instability after further machining. In section IV, the stresses decrease to -27.3 MPa, indicating structural instability and variability in response to machining in less rigid areas.

In shaft 3, the average compressive stresses in section II are significantly lower equal approx. -195.8 MPa during the first phase of machining, which may indicate the presence of defects that weaken the shaft in this section. The high compressive stresses in sections I equal approx. -478.5 MPa and IV equal approx. -325.8 MPa suggest greater stiffness and less influence of defects at these locations. After the second machining phase, the stresses in section II change to high tensile equal approx. 689.0 MPa, indicating instability due to the presence of internal defects. In section I, high tensile stresses equal approx. 649.5 MPa are observed, suggesting the influence of internal defects on deformation at locations closer to the edge of the shaft.

In shaft 4, without internal defects, the average compressive stresses are evenly distributed and predictable in the first phase of machining, especially in sections I equal approx. -410.8 MPa and IV equal approx. -543.3 MPa, indicating the absence of internal defects. In section II, the higher average compressive stresses equal approx. -668.8 MPa may be due to a more complex stress distribution resulting from the shaft geometry, but without the influence of defects. The higher value of compressive stresses in this section of the shaft indicates its high stiffness. In the second machining phase, the average stresses in section II decrease to -298.8 MPa (still compressive), showing a more predictable stress dissipation after subsequent machining. This situation is different to the shafts that are identified as internally defective shafts. Section IV shows minimal stress changes 23 MPa with a very small standard deviation, indicating structural stability and no influence of defects.

The stress values presented above in the different planes of the shaft section are average values. The values in sections I–IV will be discussed below in terms of the angular position of the measuring point on the circumference of the shaft. These values may indicate the presence of local plastically altered areas resulting from the peculiarities of the forging process. For shaft 1, the highest residual stress equal approx.  $-450 \pm 5$  MPa is found in section IV at point 2. In contrast, the lowest stress equal approx.  $-190 \pm 4$  MPa is found in section II at point 1. For shaft 2, the highest residual stress equal approx.  $-786 \pm 3$  MPa is found in section IV at point 2. The lowest stress equal approx.  $-169 \pm 7$  MPa occurs in section I at point 3. The highest residual stress in shaft 3 equal approx.  $-565 \pm 4$  MPa occurs

in section I at point 3. The lowest stress equal approx.  $-142 \pm 7$  MPa occurs in section III at point 1. For shaft 4, the highest residual stress equal approx.  $-630 \pm 6$  MPa is located in section III at point 4. The lowest stress equal approx.  $-97 \pm 7$  MPa occurs in section II at point 1. Residual stresses are stresses that remain in the material even after the cause of their origin has been removed. They may result from various mechanisms, such as inelastic deformation, temperature gradients or structural changes. In some cases, residual stresses can lead to significant plastic deformation, causing warpage and distortion of the object. In other cases, they affect the susceptibility to fracture and fatigue.

In the context of the results, residual stress values can affect the strength and durability of shafts. For example, shaft 2 shows the highest residual stress equal approx.  $-786 \pm 3$  MPa in section IV at point 2, which may suggest that this part of the shaft may be more susceptible to cracking or failure. On the other hand, shaft 4 shows the lowest residual stress equal approx.  $-97 \pm 7$  MPa in section II at point 1, which may suggest that this part of the shaft may be more resistant to cracking or damage.

## 4 Conclusions

Based on the results presented, conclusions can be drawn indicating a correlation between residual stresses on the surface of forged shafts and the occurrence of internal defects in them. The machining process reveals internal defects through changes in the distribution of residual stresses. Shafts with defects tend to shift from compressive to tensile stresses in the more deformable areas (section II), leading to structural instability when further layers of material are removed. In shafts without internal defects, the residual stresses in the shaft remain more stable and predictable, both after the first and second machining phases. The smaller stress changes in cross-sections I and IV indicate a uniform stress dissipation and no influence of internal defects on the machining process.

A comparison of the residual stresses and the location of the defects should be taken into account. Based on the results obtained, it is crucial to further develop computational models for a deeper interpretation and understanding of stresses in materials. The integration of measurement results with numerical modelling, such as the finite element method (FEM), can significantly contribute to the development of new strategies to minimise the negative effects of residual stresses on the mechanical properties of materials.

Residual stress measurements can provide valuable information that can help predict cracking in materials. Residual stresses are the stresses that remain in a material after an external load has been removed. Particular attention should be paid to the shape of the



graphs showing the level of residual stresses in characteristic sections of shafts with internal defects after the second machining phase. The diagram takes the shape of an inverted 'U'. This shape is closely related to the loss of stiffness of the shafts after machining. Lower residual stresses are observed in shaft sections that are closer to the clamping points, while higher stresses are observed where a loss of stiffness is expected due to internal shaft defects.

Residual stresses can have both positive and negative effects. On the one hand, residual stresses can increase fatigue strength and crack resistance. On the other hand, if the residual stresses are too high, they can lead to undesirable deformation and cracking.

The analysis of residual stresses in forged shafts makes it possible to effectively identify internal defects by observing the distribution of compressive and tensile stresses and their changes after successive machining phases. At the same time, it should be emphasised that measurement with an X-ray diffractometer is a time-consuming process and requires specialised knowledge and technical equipment. Shafts with internal defects show much greater stress instability, particularly in the central sections, which leads to difficulties in precise machining and increases the risk of damage during operation. In contrast, a shaft without defects has a more consistent and predictable stress distribution, highlighting its better structural integrity and stability during machining. Analysis of these differences is crucial for defect diagnosis and quality assessment in forged shafts.

## Acknowledgement

*This work was prepared within the project PM/SP/0064/2021/1 titled 'Intelligent measurement techniques in the diagnosis and forecasting of shaft cracks and their dimensional and shape accuracy, financed by the Ministry of Education and Science (Poland) as a part of the Polish Metrology Programme.*

## References

- [1] SINGH A., AGRAWAL A. (2015). Investigation of surface residual stress distribution in deformation machining process for aluminum alloy. *Journal of Materials Processing Technology*, Vol. 225, No. 4, pp. 195–202.
- [2] JU K., DUAN C., SUN Y., SHI J., KONG J., AKBARZADEH A. (2022). Prediction of machining deformation induced by turning residual stress in thin circular parts using ritz method. *Physica A: Statistical Mechanics and its Applications*, Vol. 307, 117664.
- [3] HAŁAS W. (2010). Badanie wpływu naprężeń szczątkowych na dokładność wytwarzania wałów. Rozprawa doktorska, 1-141. URL: <https://bc.pollub.pl/Content/660/PDF/d248.pdf>
- [4] EL-HASSAR F.Y., EL AJRAMI M., MILOUKI H., MEGUENI A. (2017). Effect Of Machining Parameters On Residual Stresses Distribution. *Australian Journal of Basic and Applied Sciences*, Vol. 11, No. 5, pp. 196-201.
- [5] MASOUDI S., AMINI S., SAEIDI E., et al. (2015). Effect of machining-induced residual stress on the distortion of thin-walled parts. *International Journal of Advanced Manufacturing Technology*, Vol. 76, pp. 597–608. <https://doi.org/10.1007/s00170-014-6281-x>
- [6] ZIENKIEWICZ O.C., BATHE K.J. (2005). Forming, during which various structural defects, e.g. collapses, can be generated that are difficult to detect.
- [7] HAŁAS W. (2010). Badanie wpływu naprężeń szczątkowych na dokładność wytwarzania wałów. Rozprawa doktorska, 1-141. URL: <https://bc.pollub.pl/Content/660/PDF/d248.pdf>
- [8] EL-HASSAR F.Y., EL AJRAMI M., MILOUKI H., MEGUENI A. (2017). Effect Of Machining Parameters On Residual Stresses Distribution. *Australian Journal of Basic and Applied Sciences*, Vol. 11, No. 5, pp. 196-201.
- [9] YOUNG K., NERVI S., SZABO B. (2005). Machining-Induced Residual Stress and Distortion. *SAE Technical Paper*, 2005-01-3317. <https://doi.org/10.4271/2005-01-3317>
- [10] YUE C., GAO H., LIU X., LIANG S.Y. (2018). Part Functionality Alterations Induced by Changes of Surface Integrity in Metal Milling Process: A Review. *Applied Sciences*, Vol. 8, 2550. DOI: <https://doi.org/10.3390/app8122550>
- [11] FELHŐ, C., SZTANKOVICS, I., MAROS, Z., KUN-BODNÁR, K. (2023). FEM Simulation of the Flange Turning in the Production of Aluminium Aerosol Cans, pp. 810 – 818. *Manufacturing Technology*, Vol. 23, No. 6. DOI: 10.21062/mft.2023.104.
- [12] ZIENKIEWICZ O.C., BATHE K.J. (2005). Forming, during which various structural defects, e.g. collapses, can be generated that are difficult to detect.
- [13] KOWALSKI P., ZIELIŃSKI R., NOWAK K. (2018). Zastosowanie rentgenografii w analizie naprężeń w elementach maszynowych. *Engineering Materials*, Vol. 38, No. 3, pp. 212-219.

- [14] WOZNIAK A., ZIELINSKI R. (2013). Metrological challenges in modern manufacturing processes. *Measurement*, Vol. 46, No. 9, pp. 3653-3662.
- [15] DE CHIFFRE L., CARMIGNATO S., KRUTH J.P., SCHMITT R., WECKENMANN A. (2014). Industrial applications of computed tomography. *CIRP Annals*, Vol. 63, No. 2, pp. 655-677.
- [16] SCHAJER G.S. (Ed.). (2013). *Practical Residual Stress Measurement Methods*. John Wiley & Sons.
- [17] SMITH D.J. (2001). Residual stress measurement techniques. *Materials Science and Technology*, Vol. 17, No. 4, pp. 355-365.
- [18] FITZPATRICK M.E., LODINI A. (Eds.). (2003). *Analysis of Residual Stress by Diffraction Using Neutron and Synchrotron Radiation*. CRC Press.
- [19] WITHERS P.J. (2007). Residual stress and its role in failure. *Reports on Progress in Physics*, Vol. 70, No. 12, pp. 2211-2264.
- [20] NOWAK J., KOWALSKI M., WIŚNIEWSKI A. (2020). Rentgenowskie metody analizy naprężeń własnych w wałach kutyh. *Journal of Material Science*, Vol. 45, No. 6, pp. 1123-1135.
- [21] KOWALSKI P., ZIELIŃSKI R., NOWAK K. (2018). Zastosowanie rentgenografii w analizie naprężeń w elementach maszynowych. *Engineering Materials*, Vol. 38, No. 3, pp. 212-219.
- [22] MELLER, A., SUSZYŃSKI, M., LEGUTKO, S., TRĄCZYŃSKI, M., CERNOHLAVEK, V. (2023). Studies on a Robotised Process for Forging Steel Synchronizer Rings in the Context of Forging Tool Life, pp. 88 – 98. *Manufacturing Technology*, Vol. 23, No. 1. DOI: 10.21062/mft.2023.002.
- [23] DE CHIFFRE L., CARMIGNATO S., KRUTH J.P., SCHMITT R., WECKENMANN A. (2014). Industrial applications of computed tomography. *CIRP Annals*, Vol. 63, No. 2, pp. 655-677.
- [24] PHILLIPS S.D., ESTLER W.T. (2011). A metrology system for production geometry assurance. *Precision Engineering*, Vol. 35, No. 1, pp. 48-58.
- [25] HAŁAS W. (2010). Badanie wpływu naprężeń szczątkowych na dokładność wytwarzania wałów. Rozprawa doktorska, 1-141. URL: <https://bc.pollub.pl/Content/660/PDF/d248.pdf>
- [26] KOZOVÝ, P., ŠAJGALÍK, M., DRBÚL, M., HOLUBJÁK, J., MARKOVIČ, J., JOCH, R., BALŠIANKA, R. (2023). Identification of Residual Stresses after Machining a Gearwheel Made by Sintering Metal Powder, pp. 468 – 474. *Manufacturing Technology*, Vol. 23, No. 4. DOI: 10.21062/mft.2023.054.
- [27] TIMÁROVÁ, L., KRBAŤA, M., KOHUTÍAR, M., ESCHEROVÁ, J., JUS, M. (2024). Experimental Study of Tool Life Depending on Cutting Speed for 100CrMn6 Materials & Statistical Processing Using Linear Regression Analysis, pp. 448 – 457. *Manufacturing Technology*, Vol. 24, No. 3. DOI: 10.21062/mft.2024.044.
- [28] MARDONOV, U., KHASANOV, S., JELTUKHIN, A., OZODOVA, S. (2023). Influence of Using Cutting Fluid under the Effect of Static Magnetic Field on Chip Formation in Metal Cutting with HSS Tools (turning operation), pp. 73 – 80. *Manufacturing Technology*, Vol. 23, No. 1. DOI: 10.21062/mft.2023.006.
- [29] SZYMAŃSKI W. (2018). Measurement of residual stresses in railway axes using the X-ray method according to PN-EN 13261 + A1 2011. *Proceedings of 47th National Conference on Nondestructive Testing (KKBN)*, Kołobrzeg, Poland. DOI: 10.26357/BNiD.2018.035